Applied Thermal Engineering 213 (2022) 118636

Contents lists available at ScienceDirect

Applied Thermal Engineering

journal homepage: www.elsevier.com/locate/ate

Research Paper

Lifespan and efficiency gain for outdoor electronic systems from radiative cooling: A case study on distribution transformers

Joseph Peoples [a], Fredrik Arentz [a], Yizhou Fang [a], Carmela Mohan [a], Jie Li [b], Xiangyu Li [a], Xiulin Ruan [a,*]

[a] School of Mechanical Engineering, Purdue University, West Lafayette, IN 47907, USA
[b] Eaton Research Laboratory, Menomonee Falls, WI 53051, USA

ARTICLE INFO

Keywords:
Radiative cooling
Transformer thermal management
Passive cooling

ABSTRACT

We investigate the impact of radiative cooling (RC) on pole-type distribution transformers which are utilized daily around the world, as a case study for broad range of outdoor electrical systems that feature high internal heating and require unique cooling strategies. A majority outdoor electrical equipment, including distribution transformers, rely on passive thermal management techniques via natural convection and radiation to dissipate the internal heat generated by electrical inefficiencies. Utilizing RC paint on the exterior of the case would allow further dissipation of heat to deep-space, an infinite heat sink at 3 K, as well as increase the solar reflectance to lessen the external heat load on the equipment. A single 25 kVA pole-type transformer is modeled via CFD. Two different exterior case coatings, the standard gray coatings commonly utilized and an RC coating, $BaSO_4$ paint, are analyzed under different operating loads and ambient temperatures. The RC coating makes a 25 kVA distribution transformer's windings more than 9 K cooler than the standard case with an ambient air temperature of 321 K and demonstrates below ambient cooling of the case at low heat generations. The lifetime of the distribution transformers is increased by greater than 50% when comparing the standard paint case to the RC paint case based on the Aging Acceleration Factor.

1. Introduction

Outdoor electrical equipment, such as transformers and 5G antennas, are characterized by their internal heating and need for thermal management. Distribution transformers are an example of a common outdoor electronic system, which are utilized daily worldwide, and the subject of many research areas. However, the thermal management of these transformers have not seen major advancements in decades. In the United States, distribution transformers consume 2%–3% of the electricity generated annually due to inefficiencies, which equates to $25 billion lost [1]. These inefficiencies are broken into two categories: no load losses and load losses. The no load losses are due to the electrical imperfections of the system, whether it be from contact resistance, current leakage, or magnetic hysteresis losses. These types of losses will not be considered in this work, though they do account for 25% of the total electricity lost in a distribution transformer [1]. The load losses are primarily due to the joule heating in the system. If there were a more effective thermal management technique then the load losses could be reduced, which ultimately saves electricity and extends the life of the distribution transformer.

In order to understand the heat source and cooling mechanisms of these transformers, the components and assembly must be understood. The major components of any transformer are the core and coils, which are components responsible for transforming 7.2 kV electricity into 240 V that is utilized to power a residential building. The coils are made up of insulated copper or aluminum windings, one primary winding for the high voltage and one secondary winding for the low voltage. The core is made of laminated sheets of steel to reduce some of the losses due to eddy currents. The load losses primarily come from the coils and core due to joule heating. The entire casing is filled (minus the room for volumetric expansion due to heating) with a dielectric oil, most commonly Envirotemp FR3 [2], to help evenly distribute the heat and further electrically insulate/isolate the components. The dielectric oil serves a second purpose which is to be able to make the transformer more compact as it has a lower electrical conductivity than air, meaning high voltage devices can be closer together without fear of arcing/shorting [3]. There are two major design criteria for distribution transformers: one, minimize the electric losses in the system; two, maximize the lifetime of the system. Both of these criteria are negatively impacted by increasing temperature; therefore, understanding

* Corresponding author.
E-mail address: ruan@purdue.edu (X. Ruan).

https://doi.org/10.1016/j.applthermaleng.2022.118636
Received 23 October 2021; Received in revised form 14 March 2022; Accepted 5 May 2022
Available online 20 May 2022

and optimizing the heat flow in the system is imperative to engineer more efficient, longer lasting distribution transformers.

Distribution transformers have highly dynamic loading profiles. This leads to large temperature rises in the laminated magnetic core and the cellulose polymer coated windings. The cellulose polymer deteriorates more rapidly with an increase in temperature. The manufacture will rate the life of the transformer based on the hot spot temperature (HST), which is the maximum temperature in the winding and most manufactures estimate the life of a 25 kVA transformer using a HST of 90 ° C [4]. Anything above the 90 ° C will drastically decrease the life of the transformer, this will be discussed in more detail in the Methods section [4].

Abdullah-Al-Imran et al. developed a model to analysis the load losses for both copper and aluminum conductors for various three-phase distribution transformer [5]. Keon-Je et al. numerically modeled the natural convection inside a single-phase oil immersed distribution transformer, including the effects of turbulence within the oil [6]. Hajidavalloo et al. quantifies the thermal effects of solar irradiation on distribution transformer experimentally and demonstrate the utility of a solar shield [7]. They demonstrated that with the use of a solar shield the transformer life can increase by up to 24% and lower the core temperature up to 7 °C. Though Hajidavalloo used a solar shield, these results can also be used to show the benefits of the radiative cooling coating because it must reflect all incoming solar irradiation to cool the surface. Shiri et al. investigated the effects of the ambient temperature on insulation life of high power, 180 MVA transformers [8]. They showed that an average ambient temperature increase of 11 °C can decrease the life of the transformer by 2.5 times [8].

These works show the importance of loading and temperature on the transformer's efficiency and lifetime. However, the benefits of RC on outdoor electrical equipment, such as 5G antennas or distribution transformers, have yet to be analyzed. Radiative cooling (RC) is an emerging passive thermal management technology that has been extensively studied for building applications [9–13]. It is a passive cooling technique which requires engineering the optical properties of a surface to obtain high solar reflectivity while simultaneously achieving high mid-infrared emissivity. Several works published different types of coatings that could achieve 24 hr below ambient, passive radiative cooling [14–17]. Most of these solutions rely on a metallic bi-layer or complex crystalline structure to achieve the desired optical surface which are not applicable for many outdoor electronic systems, including distribution transformers, due to high electrical conductivity or the complex manufacturing techniques needed to apply the coatings. Recently, our group developed radiative cooling paints that are an inexpensive, easily-scalable, and metal-free solution with high cooling performance [18–20]. Radiative cooling paints are an ideal passive cooling method for pole-type distribution transformers that currently rely on natural convection from the exterior of the case. Furthermore, radiative cooling paints can be an easy retrofit on to existing outdoor electrical equipment, such as transformers, with ease to create a more efficient power grid with very little cost.

In this investigation, passive radiative cooling of a 25 kVA single-phase overhead distribution transformer will be analyzed. The buoyancy driven flow and temperature rise of various heat generation rates will be solved using a CFD model to simulate the conjugate heat transfer within the case. Two different exterior case coatings were simulated: one with the traditional gray paint and the other utilized our novel radiative cooling paint. We study the benefits of radiative cooling to create a more efficient transformer by decreasing the temperature, thereby decreasing the resistivity, of the system to minimize the load-losses and extend the life of the transformer.

2. Methods

2.1. Design and thermophysical properties

In order to quantify the enhancement of the radiative cooling (RC) of a 25 kVA distribution transformer two models are developed. The two models have compared the effects of traditional transformer paint, i.e. gray paint, and radiative cooling paint, i.e. $BaSO_4$ white paint, as seen in Fig. 1. There are four heat rejection pathways considered in these models. First is the extraterrestrial radiation, Q_{RC}, which is the radiation of the paints to deep-space, an infinite heat sink at 3 K. Then we consider the terrestrial radiation term, Q_{terr} which is the radiation to objects at ambient temperature such as the ground, trees, buildings, or telephone poles. The absorbed solar irradiation, $(1 - \rho_{solar})G$, on the surface is a heat gain that is considered on the exterior of the surface. Lastly the convective heat transfer Q_{conv} calculated by the natural convection between the surface temperature and ambient temperature is considered.

Due to the complex nature of the buoyancy driven flow for concentric cylinders of different heights in high Prandtl number dielectric oil, this work implements CFD to solve for the conjugate heat transfer using ANSYS Fluent [21]. In Fig. 2, the simplified geometry used in the CFD is shown. The scope of this work is to analyze the benefits of RC utilizing known numerical techniques coupled with validated heat transfer models; rather than creating the most accurate single-phase distribution transformer model with individual winding wires and accurate high-voltage joule heating effects.

The windings, shown in Fig. 2, are modeled as a bulk copper block with a uniform heat generation, and the two cores are modeled as bulk carbon-steel blocks. The core is assumed to be in contact with the bottom of the case so the heat can be conducted or convected to the case either through the core or the FR3 dielectric oil, respectively. Taking the load losses published by Abdullah-Al-Imran et al. for the 25 kVA transformer into consideration [5], this investigation will analyze all the heat dissipation at steady state, while varying the uniform heat generation in the windings from 50 to 700 W in 50 W increments.

All intrinsic thermophysical properties will be assumed to be constant across the whole temperature range for the fluid domain and are listed in Table 1. The fluid domain is modeled as Envirotemp FR3 and the properties listed in Table 1 are from Envirotemp [2]. The properties for the solid domains are taken from Fluent's database [21]. The uniform volumetric heat generation is applied to the windings. When solving for the thermal radiation, the case is separated into three independent surfaces: the top, side, and bottom with the condition that the temperatures must match at the boundary of each surface. The terrestrial view factor, which is the radiation from the case to objects at ambient temperature. The RC view factor is only applicable for the extraterrestrial, i.e. radiative cooling, heat flux; the bottom of the case has an RC view factor of zero and the top of the case is assumed be unity as it has a clear view of sky/deep-space. The view factor for the side surface is more complex, if one distribution transformer is mounted to a pole with no other high rises around then the view factor can be calculated using Juul's formulation presented below in Eqs. (1)–(4) [22].

$$Y = \frac{r_2}{r_1} \tag{1}$$

$$S = \frac{s}{r_1} \tag{2}$$

$$C = 1 + Y + S \tag{3}$$

$$\begin{aligned} F_{1-sur} = 1 - \frac{1}{2\pi}\Big(&\pi + \left[C^2 - (Y+1)^2\right]^{1/2} \\ &- \left[C^2 - (Y-1)^2\right]^{1/2} \\ &+ (Y-1)\cos^{-1}\left[\left(\frac{Y}{C}\right) - \left(\frac{Y}{C}\right)\right] \\ &- (Y+1)\cos^{-1}\left[\left(\frac{Y}{C}\right) + \left(\frac{Y}{C}\right)\right]\Big) \end{aligned} \tag{4}$$

where r_1 and r_2 are the radii of the transformer and pole respectively, s is the distance between the transformer and the pole, F_{1-sur} is the view factor from the transformer to deep space [22]. Using this view factor solution neglects the differences in the axial direction of the

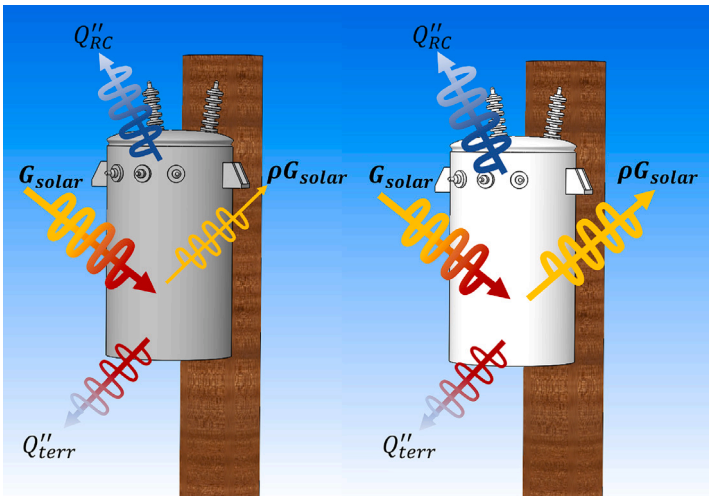

Fig. 1. Concept figure to illustrate the two cases studied. The first transformer has the traditional gray paint with moderate solar reflectance coupled with high mid-IR emittance and the second transformer has RC paint with high solar reflectance coupled with high mid-IR emittance.

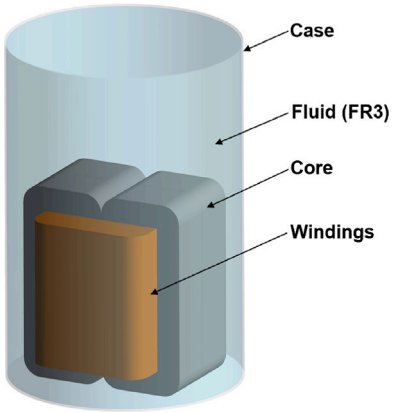

Fig. 2. Geometry utilized in CFD simulations, the windings are copper, the core is made of carbon steel, the fluid is FR3 dielectric oil, and the case is made of aluminum.

Table 1
Thermophysical properties utilized in the model.

Fluid: Envirotemp FR3 (Ref. [2])		
Thermal Conductivity [W/(m K)]		0.167
Specific Heat [J/(kg K)]		1882.8
Kinematic Viscosity at 20 °C [m/s^2]		$3.3 \cdot 10^{-5}$
Prandtl Number [-]		340.5
Density [kg/m^3]		919.2
Windings: Copper		
Thermal Conductivity [W/(m K)]		387.6
Specific Heat [J/(kg K)]		381
Density [kg/m^3]		8978
Resistivity of 6 mm^2 wire at 20 °C [Ω/km]		3.28
Resistivity Temperature Coefficient [1/K]		$4.29 \cdot 10^{-3}$
Core: Carbon Steel		
Thermal Conductivity [W/(m K)]		60.5
Specific Heat [J/(kg K)]		434
Density [kg/m^3]		7854
Case: Aluminum		
Property	Std	RC
Thermal Conductivity [W/(m K)]	202.4	
Specific Heat [J/(kg K)]	871	
Density [kg/m^3]	2719	
Solar Reflectance [-]	0.25	0.963
Solar View Factor (T/B/S) [-]	1/0/0.4	1/0/0.4
Mid-IR Emittance [-]	0.95	0.95
Terrestrial View Factor (T/B/S) [-]	0/1/0.11	0/1/0.11
RC View Factor (T/B/S) [-]	1/0/0.89	1/0/0.89

transformer, but due to the altitude of the transformer compared to its overall length this assumption is warranted. The solar reflectance of the Standard case is assumed to be 0.25 which is common for gray paints [23], while the RC solar reflectance corresponds to that of the novel $BaSO_4$ RC paint developed in our lab [20]. The solar reflectance of the paint can vary in the range of 96–98.1% for different batches of preparation and nanoparticles, and some typical values measured by third parties and us are 98.1%, 97.6%, and 96.3%. In this work, 96.3% is used in the simulation as a conservative estimation of the radiative cooling benefits.

2.2. Numerical methods and boundary conditions

Due to the complex nature of the buoyancy driven flow in a high Prandtl number fluid, ANSYS Fluent was implemented to solve for the heat transfer within the case [21]. The ANSYS Fluent theory guide goes into great depth on the governing equations and numerical solution techniques implemented in the software so we will not go into a detailed explanation in this work [24]. The FR3 fluid domain was considered to be an incompressible ideal gas. The Rayleigh number for the highest heat generation inside the fluid domain for the closest distance between two vertical surfaces was Ra= $8.8 \cdot 10^7$, which is below the Ra = 10^9 turbulent transition for vertical plates; therefore the flow inside the case was considered to be laminar. The laminar, inviscid model was implemented as well as the energy equation. Second order, upwind numerical schemes were utilized to solve for energy and momentum, the second order scheme was implemented for pressure with pressure velocity coupling [24]. All the default under-relaxation factors were preserved [21]. To ensure accurate solutions the convergence conditions were set to $< 10^{-5}$ for continuity and all velocity components, as well as $< 10^{-9}$ for the energy equation. Furthermore, additional convergence criteria was implemented based on temperature, the area-weighted average surface temperatures for the top, bottom, and sides of the case all must converge to $< 10^{-5}$ and the volume-weighted average of the windings was also set to converge at $< 10^{-5}$.

The boundary conditions for natural convection to the ambient air and radiation effects on the exterior of the case were solved with two custom User Defined Functions (UDFs): one for the Standard Case and one for the RC case. The natural convection boundary condition is chosen as this is the worst thermal scenario for a distribution transformer

under load that is passively cooled to the ambient air. Furthermore, we assume a clear-sky with solar irradiation of 800 W/m^2 and a clear line of sight to the horizon as many rural transformers are not hindered by high rise structures. The natural convection to the ambient air accounts for temperature dependent thermophysical properties of air at 1 atm. The UDFs solve for the heat flux at each discretized surface element on the exterior of both cases with the implementation as a heat flux boundary condition in Fluent [21]. The discretized surface elements are all < 1 cm in length, equating to thousands of surface elements on each exterior boundary to fully resolve the thermal effects of the system. The difference in the two UDFs are based on the material properties described in Table 1. The heat flux on the top, bottom, and side surfaces of the case only differ by the Nusselt number correlation utilized and the view factors for the RC flux. The Nusselt number correlation for the bottom surface is given by [25],

$$Nu_{b-a} = 0.27\, Ra_{D,a}^{1/4} \tag{5}$$

which is valid for $\mathrm{Ra}_{D,a}$ from 10^5 to 10^{11} and $Ra_{D,a}$ is the Rayleigh number for the diameter of the case. For reference, the generic equation for Rayleigh is given by,

$$Ra_{Lc} = Pr\, Gr_D = \frac{g\,\beta\,(T_s - T_a)\,Lc^3}{\nu\,\alpha} \tag{6}$$

where g is gravity, β is the inverse of the film temperature, Lc is the characteristic length, ν is the kinematic viscosity, and α is the thermal diffusivity. The side surface of the case can be approximated as a vertical flat plate since $D > 35L/Gr_L^{1/4}$, from there the Nusselt number correlation for vertical plate approximation for the entire range of Rayleigh numbers is [25],

$$Nu_{s-a} = \left[0.825 + \frac{0.387\, Ra_{L,a}^{1/6}}{\left[1 + \left(0.492/Pr_a\right)^{9/16}\right]^{8/27}}\right]^2 \tag{7}$$

where Pr_a is the Prandtl number of the air, and $Ra_{L,a}$ is the Rayleigh number for the height of the case. The Nusselt correlation utilized for the top of the case is,

$$Nu_{t-a} = 0.54\, Ra_{D,a}^{1/4} \tag{8}$$

which is valid from 10^4 to 10^7. Once the Nusselt number is known, the convective heat transfer coefficient can be found from $h = Nu\, k_a/d$. The radiation to deep-space is calculated from,

$$P_{LWR}(T_s) = \int_0^{\pi/2}\int_0^{\infty} 2\pi \sin(\theta)\cos(\theta)\, I_{bb}(T_s,\lambda)\,\varepsilon_s(\lambda,\theta)\, d\lambda\, d\theta \tag{9}$$

$$I_{bb}(T,\lambda) = \frac{2\hbar c_0^2}{\lambda^5\left[exp\left(\frac{\hbar c_0}{\lambda T k_B}\right) - 1\right]} \tag{10}$$

where T_s is the surface temperature, $\varepsilon_s(\lambda,\theta)$ is the emissivity of the surface, and I_{bb} is the black body spectral intensity calculated with Planck's constant, $\hbar$, the speed of light in vacuum, c_0, and Boltzmann's constant, k_B [26,27]. Then we calculate the amount of thermal irradiation coming from the atmosphere and absorbed by the surface, P_{atm}, using

$$P_{atm}(T_{amb}) = \int_0^{\pi/2}\int_0^{\infty} 2\pi \sin(\theta)\cos(\theta)\, I_{bb}(T_{amb},\lambda)\,\varepsilon_s(\lambda,\theta)\,\varepsilon_{atm}(\lambda,\theta)\, d\lambda\, d\theta \tag{11}$$

where T_{amb} is the ambient temperature and $\varepsilon_{atm}(\lambda,\theta)$ is the atmospheric emittance. Lastly, we calculate the net radiation leaving the surface, P_{rad}, by,

$$P_{rad} = P_{LWR}(T_s) - P_{atm}(T_{amb}) \tag{12}$$

While Eqs. 9–(12) are the most accurate method for calculating the thermal radiation from the RC paint it would be extremely computationally expensive to evaluate these integrals numerically at every computational node on the exterior of the case. Li et al. fit the experimental cooling power data from an outdoor cooling test for the BaSO4 paint using a feedback heater which matches the ambient temperature to the sample temperature and measures the voltage and amperage required to maintain the RC surface at the ambient temperature [20]. Measuring the cooling power with this technique removes any losses from natural convection as there is no temperature difference between surface and ambient. The derived temperature coefficient accounts for the extraterrestrial radiative heat flux and is a factor of sky clearness, as well as humidity. The temperature coefficient was calculated based on the nighttime cooling power to negate any solar irradiation effects. Therefore, we can accurately model the net radiative heat flux of the RC paint without the computational expense using their model below,

$$P_{rad} = 1.643 \cdot 10^{-8} * T_s^4 \tag{13}$$

which has good agreement with both the theoretical calculations and experimentally measured cooling performance [20]. Combining all the convective heat flux, the radiative cooling heat flux, and the terrestrial radiation heat flux yields the total exterior surface heat flux as,

$$q_i''(T_s) = F_{i,RC}\, P_{i,rad} - h_i\,(T_a - T_s) - F_{i,terr}\,\varepsilon_{terr}\,\sigma\,(T_a^4 - T_s^4) - F_{i,solar}\,(1-\rho_{solar})\,G_{solar} \tag{14}$$

where $F_{i,terr}$ is the terrestrial view factor for the ith surface, ε_{terr} is the terrestrial mid-IR emittance, σ is the Stephan Boltzmann constant, $F_{i,RC}$ is the RC view factor for the ith surface, $F_{i,solar}$ is the solar view factor for the ith surface, ρ_{solar} is the total solar reflectance, and G_{solar} is the solar irradiation in terms of W m^{-2}. For all the simulations done in this work, the ambient air temperature was T_a = 293 K and G_{solar} = 800 W m^{-2} to represent a standard day with mild sun.

2.3. Efficiency and lifetime analysis

Once the winding temperature is calculated, there are two ways to quantify the improvement of the RC case: the change in resistance of the core and the Aging Acceleration Factor (F_{AA}) for the winding insulation.

A distribution transformer is made of two windings and a core, as previously discussed, the primary winding that is connected to the high voltage line uses a smaller gauge copper wire with more winds than the secondary winding. There is usually a 2% impedance in the windings and the winding ratios are commonly between 25:1–30:1, therefore the major resistance is on the primary winding [5]. The increase in resistance due to temperature will be calculated using Eq. (15),

$$\Delta R = R_i \alpha_R \Delta T \tag{15}$$

where R_i is the initial resistance, α_R, is the resistivity temperature coefficient, and ΔT is the temperature difference.

The major mode of failure for a distribution transformer is the insulation deterioration due to polymer oxidation which is greatly accelerated with an increase in temperature. In order to quantify this effect, we utilized IEEE C57.91-1995, which is an IEEE standard for a modified Arrhenius equation fit to the material properties of the insulating polymer material, and is known as the Aging Acceleration Factor equation given by,

$$F_{AA} = exp\left[\left(\frac{15000}{T_{HST}}\right) - \left(\frac{15000}{T_{windings}}\right)\right] \tag{16}$$

where T_{HST} is the rated hot spot temperature for the transformer in Kelvin and $T_{windings}$ is the core temperature in Kelvin [4]. The rated hot spot temperature for this work is assumed to be 363 K based on commercial transformers [3]. If $F_{AA} = 1$ then the transformer will last the manufacturer rated lifetime, if $F_{AA} < 1$ then it will last longer, and if $F_{AA} > 1$ then the lifetime is reduced by that factor.

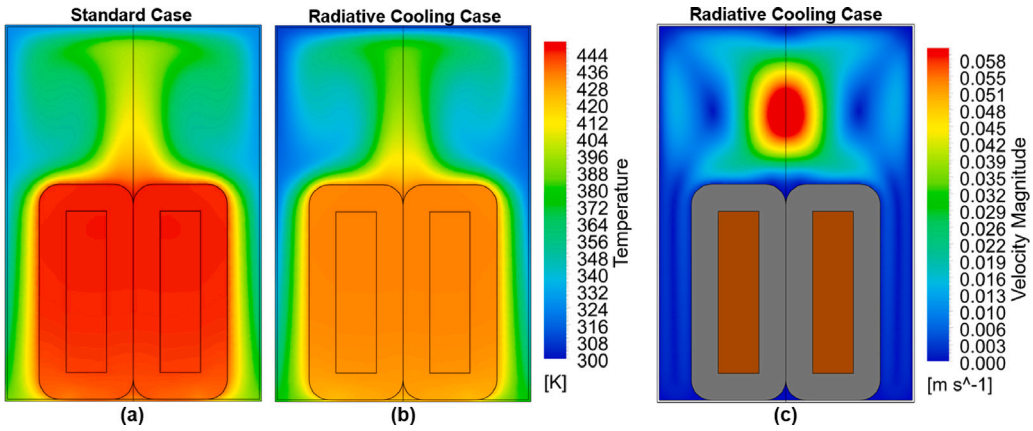

Fig. 3. Temperature contours for the 700 W heat generation along the YZ symmetry plane for (a) the Standard case and (b) the RC case. (c) Velocity magnitude contour for the 700 W heat generation along the YZ symmetry plane for the RC case.

3. Results and discussion

The two cases were each simulated for the same 14 heat loads ranging from 50 W to 700 W by applying a uniform heat generation in the windings. All the thermal results for the case surfaces are based upon the area-weighted average for each respective surface, and the thermal results for the windings are based upon the volume-weighted average of the copper. Comparing the volume-weighted average to the maximum body temperature yielded a difference of >0.2 K for the highest heat generation which had the greatest thermal gradient, and since this work utilized a bulk copper block for the windings at steady-state the differences were negligible. Actual windings that are made up of a complex composition of copper wire, polymer coatings, and paper insulation have a greater thermal gradient throughout the system. The scope of this work is not to create the most accurate thermal model for transformers, but to quantify the benefits of utilizing an RC paint on the case.

In Figs. 3a–c an example of the temperature and velocity contours are presented for the 700 W heat generation. Fig. 3a shows the temperature contour in the middle of the transformer along the YZ symmetry plane for the Standard case while Fig. 3b is for the RC case, and they share a common temperature scale to better visualize the results. Notice that the windings and core are approximately 11 K cooler with the RC case. Fig. 3c is a contour of the velocity magnitude in the fluid domain, which illustrates the recirculating buoyancy driven flow of the FR3 fluid. These contours are presented to give context to the temperature profiles presented in the latter results of this work.

3.1. Winding temperature

In Fig. 4a the volume-weighted average winding temperature is shown as a function of heat generation at an ambient temperature of 293 K. The red triangles represent the Standard case and the blue circles represent the RC case. The temperature decrease with the RC case is mainly attributed to the lower solar absorptance of the exterior of the case compared to the Standard case. At the lower heat generations there is a larger benefit because the RC case is actually being cooled below the ambient temperature. The below ambient cooling of the case is shown in Fig. 4b at 293 K ambient, where the area-weighted average surface temperatures are shown. The 50 to 150 W heat generation produces below ambient cooling for the top of the RC case, and 50 to 100 W heat generation show below ambient cooling of the side of the case. Fig. 4c illustrates the effects of different ambient temperatures on the windings, the trends are very linear over different heat loads. The three temperatures were chosen based on the coldest (272 K) and hottest (321 K) recorded temperatures in Reno, NV in 2018 and a mild temperature (293 K). Reno, NV was selected as the location because this is where the $BaSO_4$ paint was experimentally characterized in a previous work by Li et al. [20]. Fig. 4d is the temperature difference between the Standard case and the RC case as a function of heat load for three ambient temperatures. From Fig. 4c demonstrating the linear trends of the ambient temperatures, Fig. 4d can establish an operational window between 272 K and 321 K for any ambient temperature between these points at the respective load.

3.2. Efficiency and lifetime improvement

The temperature profiles show that the radiative cooling coating is indeed beneficial, but in order to further quantify these improvements the resistivity and Aging Acceleration Factor are presented. In Fig. 5a the change in resistance due to temperature rise (calculated using Eq. (15)) of the windings is shown for each case at an ambient temperature of 293 K and the resistance decrease due to radiative cooling is presented in Fig. 5b for ambient temperatures of 272 K, 293 K, and 321 K, respectively. While Fig. 5a shows the resistance rise as a function of heat generation for each scenario and it demonstrates that the radiative coating has some benefits, the increase in resistance for both cases is small. Fig. 5b is the resistance difference between the Standard and RC case which more clearly illustrates the potential electricity savings at a wide range of ambient temperatures. Though the resistivity savings are not large, this is a rough estimate based on a 6 mm^2 cross-sectional area and it is shown in Ω/km as the exact amount of energy savings depends on the number of turns and size of wire utilized in the transformer's primary and secondary windings.

The main cause for transformer failure is the polymer degradation on the primary and secondary winding wires which is highly sensitive to temperature. The Aging Acceleration Factor, calculated using Eq. (16), is shown in Fig. 6a which is representative of the polymer's lifetime decrease with respect to temperature at an ambient temperature of 293 K. After 250 to 300 W of heat generation the winding temperature goes above the rated HST of 363 K for the transformer which accelerated the aging effect. While these loads are common in transformers, it is not common for a transformer to sustain a 700 W load for an extended period of time, such that it reaches steady state. So while this model illustrates the benefits of the RC case, it does not capture the "real-world" physics.

To further illustrate the improvements of the RC case, the Life Gain from the Aging Acceleration Factor is shown in Fig. 6b. The RC case will create > 55% life gain for the transformer. It should be reiterated that these calculations are done under the assumptions of a clear sunny sky, constant ambient temperature of 293 K, with no high rise structures blocking the transformers view of deep space. All these factors will impact the performance of the RC case.

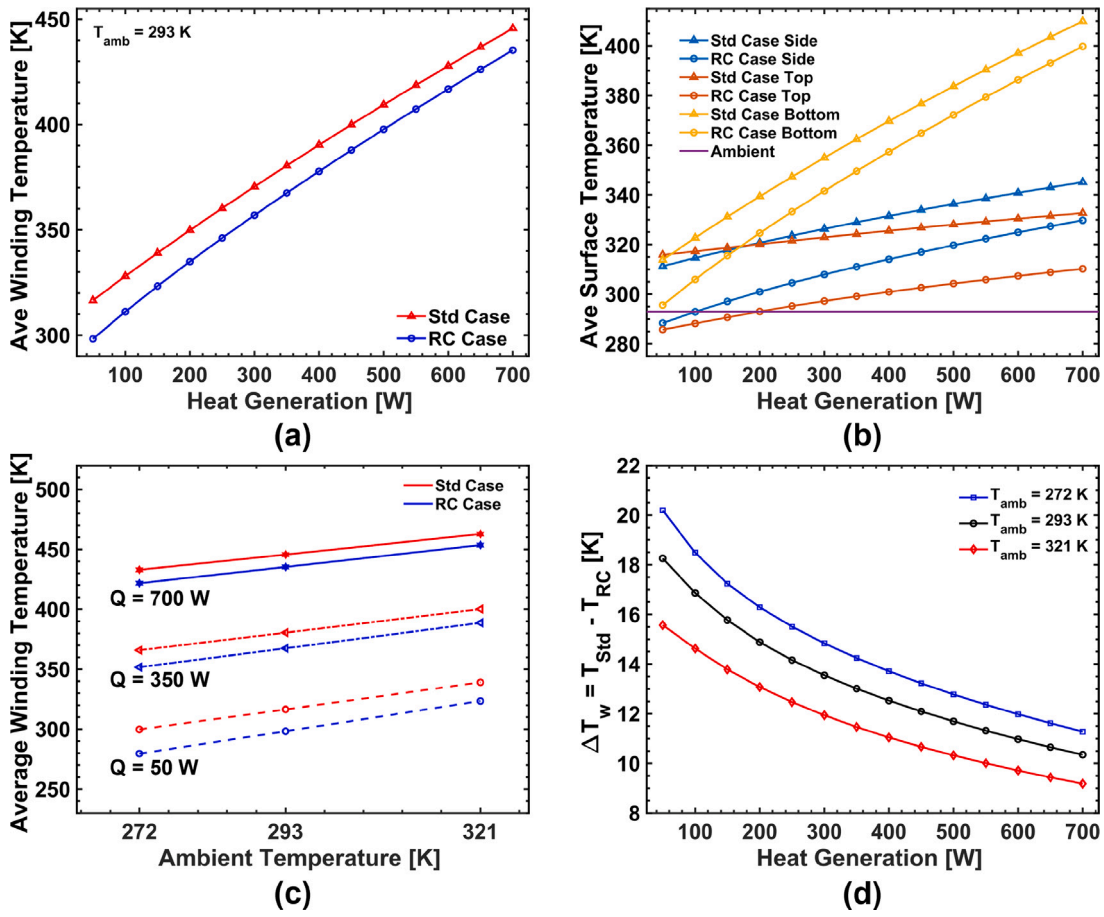

Fig. 4. (a) The volume-weighted average winding temperature as a function of heat generation for both the Standard case (triangles) and RC case (circles) at an ambient temperature of 293 K. (b) The area-weighted average surface temperatures for the side (blue line), top (orange line), and bottom (yellow line) for the Standard Case (triangles), the RC case (circles), and the purple line is the ambient air temperature at an ambient temperature of 293 K. (c) The volume-weighted average winding temperature as a function of ambient temperature for three fixed heat loads: 50 W (dashed circles), 350 W (dash–dot triangles), and 700 W (solid hexagons) for the Standard case (red) and RC case (blue). (d) The winding temperature difference between the Standard and RC case for three different ambient temperatures: 272 K (blue squares), 293 K (black circles), and 321 K (red diamonds).

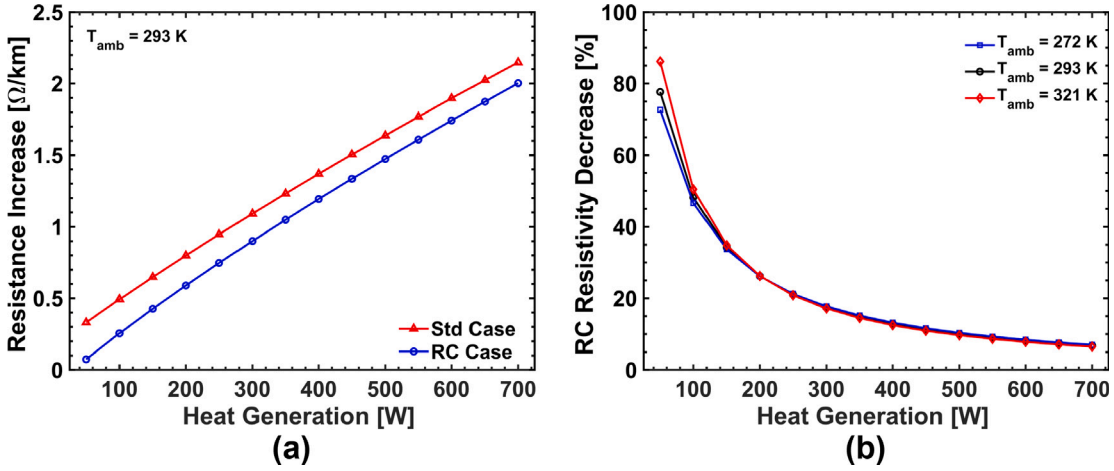

Fig. 5. (a) The resistance increase from the temperature increase in the windings, assuming a 6 mm^2 copper wire at an ambient temperature of 293 K. (b) The resistivity decrease from the RC case compared to the Standard case for three different ambient temperatures: 272 K (blue squares), 293 K (black circles), and 321 K (red diamonds).

4. Conclusion

An investigation of passive radiative cooling was conducted on a distribution transformer. Radiative cooling yielded great benefits from the thermal management and lifetime perspectives. The radiative cooling coating cooled a 25 kVA distribution transformer's windings by > 9 K, regardless of ambient temperature. The lifetime of the distribution transformers was increased by > 55% when comparing the RC case to the Standard case at an ambient temperature of 293 K. The RC paint was able to cool the case below ambient for heat generation values < 200 W, which makes sense physically as the $BaSO_4$ paint has a cooling power of 113 W m^{-2} at 293 K [20]. While our constant

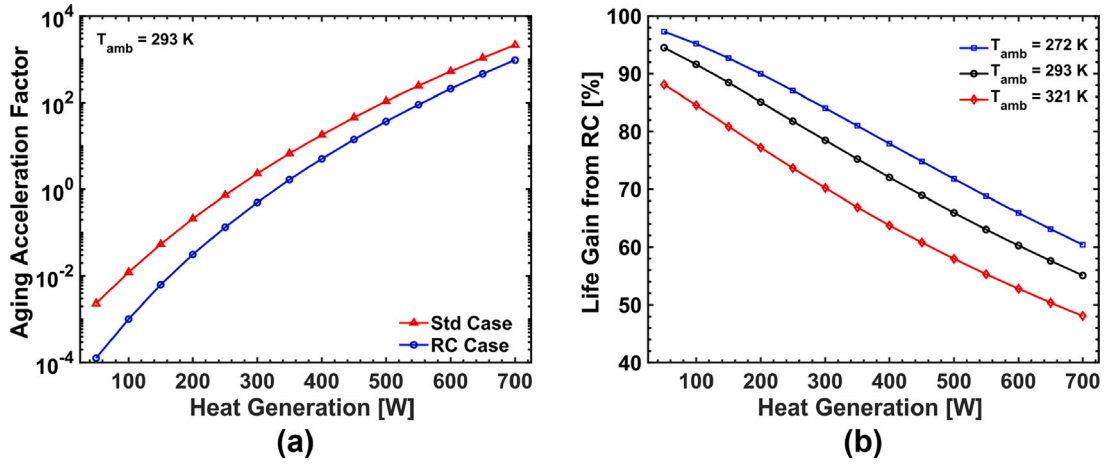

Fig. 6. (a) The Aging Acceleration Factor of both the Standard and RC case as a function of heat generation at an ambient temperature of 293 K. (b) The Life Gain from the RC case which is calculated as the percent difference between the two Aging Acceleration Factors for three different ambient temperatures: 272 K (blue squares), 293 K (black circles), and 321 K (red diamonds).

solar irradiation assumption is not realistic, the assumption does align well with the demands of the transformer, e.g. at peak solar irradiation hours, the transformers temperature is at a peak due to the building utilities requiring a high demand equating to high heat generation. Future work could consider a transient analysis with a dynamic loading curve for a 24 h period as well as more complex weather effects and a higher fidelity geometric representation.

Radiative cooling effectiveness is highly dependent on humidity, cloud coverage, and wind. For instance, when the sky is clear, radiative cooling functions more effectively while the transformers gain more solar heat and need more cooling as well. Indeed, when it is cloudy the cooling performance reduces, but the transformers will not receive an additional heat flux from solar irradiation so the cooling needs reduce as well. A detailed study of these weather effects on both the standard case and RC case is out of the scope of this work, and some relevant studies have appeared [28–30]. However, this work strongly motivates the use of RC paint on pole-type distribution transformers, as well as other outdoor electrical equipment. The life gain result alone justifies the implementation of the RC paints, as the cost of the coating is almost negligible compared to the lifetime savings. Furthermore, these results highlight the benefits of radiative cooling for exterior enclosures for many outdoor power electronics that are exposed to solar irradiation.

CRediT authorship contribution statement

Joseph Peoples: Conceived the idea, Performed the simulations, Wrote the custom UDFs, Wrote the manuscript, Commenting and editing the manuscript. **Fredrik Arentz:** Performed the simulations, Wrote the custom UDFs, Commenting and editing the manuscript. **Yizhou Fang:** Performed the simulations, Wrote the custom UDFs, Commenting and editing the manuscript. **Carmela Mohan:** Performed the simulations, Wrote the custom UDFs, Commenting and editing the manuscript. **Jie Li:** Provided experimental data and advisement for the simulations, Commenting and editing the manuscript. **Xiangyu Li:** Provided experimental data and advisement for the simulations, Commenting and editing the manuscript. **Xiulin Ruan:** Conceived the idea, Commenting and editing the manuscript.

Declaration of competing interest

The authors declare that they have no known competing financial interests or personal relationships that could have appeared to influence the work reported in this paper.

Acknowledgment

J.P. and X.R. thank the Cooling Technologies Research Center (CTRC) at Purdue University for financial support of this work.

References

[1] J. Lian, K. Burkes, Improving transformer efficiency and lifetime through product selection , system integration and dynamic control, in: DOE, Technical Report, 2018.
[2] E. FR3, ENVIROTEMP® FR3™ FLUID Brouchure, Technical Report, 2001, URL http://www.nttworldwide.com/docs/fr3brochure.pdf.
[3] Eaton, PEAK ™ Single-Phase Overhead Distribution Transformer, Technical Report August, 2015.
[4] I. Transformers, IEEE Guide for Loading Mineral-Oil- Immersed Transformers IEEE Guide for Loading Mineral-Oil- Immersed Transformers, Vol. 1995, 2003.
[5] M. Abdullah-Al-Imran, Sumon, Md. Mehedy Hasan, K.M.S. Emran, D.K. Sarker, Computer aided design and comparative study of copper and aluminium conductor wound distribution transformer, Am. J. Eng. Res. 4 (2) (2015) 133–145.
[6] K.-J. Oh, S.-S. Ha, Numerical calculation of turbulent natural convection in a cylindrical transformer enclosure, Heat Transf.—Asian Res. 28 (6) (2002) 429–441, http://dx.doi.org/10.1002/(sici)1523-1496(1999)28:6<429::aid-htj1>3.3.co;2-q.
[7] E. Hajidavalloo, M. Mohamadianfard, Effect of sun radiation on the thermal behavior of distribution transformer, Appl. Therm. Eng. 30 (10) (2010) 1133–1139, http://dx.doi.org/10.1016/j.applthermaleng.2010.01.028.
[8] A. Shiri, A. Gholami, A. Shoulaie, Investigation of the ambient temperature effects on transformer's insulation life, Electr. Eng. 93 (3) (2011) 193–197, http://dx.doi.org/10.1007/s00202-011-0202-x.
[9] S. Vall, A. Castell, M. Medrano, Energy savings potential of a novel radiative cooling and solar thermal collection concept in buildings for various world climates, Energy Technol. 6 (11) (2018) 2200–2209, http://dx.doi.org/10.1002/ente.201800164.
[10] W. Li, Y. Li, K.W. Shah, A materials perspective on radiative cooling structures for buildings, Sol. Energy 207 (July) (2020) 247–269, http://dx.doi.org/10.1016/j.solener.2020.06.095.
[11] J. Chen, L. Lu, Development of radiative cooling and its integration with buildings: A comprehensive review, Sol. Energy 212 (June) (2020) 125–151, http://dx.doi.org/10.1016/j.solener.2020.10.013.
[12] B. Zhao, M. Hu, X. Ao, N. Chen, G. Pei, Radiative cooling: A review of fundamentals, materials, applications, and prospects, Appl. Energy 236 (December 2018) (2019) 489–513, http://dx.doi.org/10.1016/j.apenergy.2018.12.018.
[13] J. Mandal, Y. Yang, N. Yu, A.P. Raman, Paints as a scalable and effective radiative cooling technology for buildings, Joule 4 (7) (2020) 1350–1356, http://dx.doi.org/10.1016/j.joule.2020.04.010.
[14] A.P. Raman, M.A. Anoma, L. Zhu, E. Rephaeli, S. Fan, Passive radiative cooling below ambient air temperature under direct sunlight., Nature 515 (7528) (2014) 540–544, http://dx.doi.org/10.1038/nature13883.
[15] A.S. Farooq, P. Zhang, Y. Gao, R. Gulfam, Emerging radiative materials and prospective applications of radiative sky cooling - a review, Renew. Sustain. Energy Rev. 144 (June 2020) (2021) 110910, http://dx.doi.org/10.1016/j.rser.2021.110910.

[16] M. Zeyghami, D.Y. Goswami, E. Stefanakos, A review of clear sky radiative cooling developments and applications in renewable power systems and passive building cooling, Sol. Energy Mater. Sol. Cells 178 (January) (2018) 115–128, http://dx.doi.org/10.1016/j.solmat.2018.01.015.

[17] S. Vall, A. Castell, Radiative cooling as low-grade energy source : A literature review, Renew. Sustain. Energy Rev. 77 (April) (2017) 803–820, http://dx.doi.org/10.1016/j.rser.2017.04.010.

[18] X. Ruan, X. Li, Z. Huang, J. Peoples, Metal-free solar-reflective infrared-emissive paints and methods of producing the same, PCT/US2019/054566, 2019, URL https://patentscope.wipo.int/search/en/detail.jsf?docId=WO2020072818&tab=PCTBIBLIO.

[19] X. Li, J. Peoples, Z. Huang, Z. Zhao, J. Qiu, X. Ruan, Full daytime sub-ambient radiative cooling with high figure of merit in commercial-like paints, Cell Rep.: Phys. Sci. 1 (10) (2020) 100221, http://dx.doi.org/10.2139/ssrn.3652325.

[20] X. Li, J. Peoples, Y. Peiyan, X. Ruan, Ultra-white BaSO4 paint and film for remarkable daytime radiative cooling, ACS Appl. Mater. Interfaces 13 (18) (2021) 21733–21739, http://dx.doi.org/10.1021/acsami.1c02368.

[21] ANSYS Academic, Fluent, ANSYS, Inc, 2020, p. R2.

[22] N.H. Juul, View factors in radiation between two parallel oriented cylinders of finite lengths, J. Heat Transfer 104 (1982) 384–388.

[23] F.E. Branch, Painting of Transformers and Circuit Breakers, Vol. 3, Technical Report November 1991, United States Department of Interior, 1991.

[24] ANSYS, Fluent Theory Guide, Technical Report, ANSYS, Inc, 2020, p. R2.

[25] A. Cengel, Yunis; Ghajar, Heat and Mass Transfer: Fundamentals and Applications, 4th, McGraw-Hill, New York, 2011.

[26] M.F. Modest, Radiative Heat Transfer, Elsevier Science, 2013, p. 882.

[27] J.R. Howell, R. Siegel, M.P. Menguc, Thermal Radiation Heat Transfer, CRC Press, Boca Raton, FL, 2016.

[28] M. Wei, W. Wu, D. Li, H. Xu, Y. Lu, W. Song, Universal strategy for all-weather and all-terrain radiative cooling with non-reciprocal mid-infrared windows, Sol. Energy 207 (July) (2020) 471–478, http://dx.doi.org/10.1016/j.solener.2020.07.010.

[29] C. Liu, Y. Wu, B. Wang, C.Y. Zhao, H. Bao, Effect of atmospheric water vapor on radiative cooling performance of different surfaces, Sol. Energy 183 (March) (2019) 218–225, http://dx.doi.org/10.1016/j.solener.2019.03.011.

[30] D. Zhao, A. Aili, Y. Zhai, J. Lu, D. Kidd, G. Tan, X. Yin, R. Yang, Subambient cooling of water: Toward real-world applications of daytime radiative cooling, Joule 3 (1) (2019) 111–123, http://dx.doi.org/10.1016/j.joule.2018.10.006.